DOI: 10.30511/pcdp.2026.2092598.1088 - ISSN: 3060-8376 - Vol 3(3), 2026

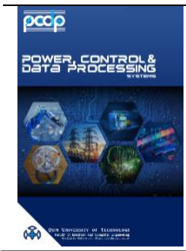

POWER, CONTROL AND DATA PROCESSING SYSTEMS

Available Online at: https://pcdp.qut.ac.ir/

An Accurate and Computationally Efficient Unit Commitment Formulation for Renewable-Integrated Power Systems

ARTICLE INFO

Article Type
Original Research

Authors
Afshin Najafi[1,*]
Abbas Vanak[1]

[1] Faculty of Electrical Engineering, K. N. Toosi University of Technology, Tehran, Iran

**** Correspondence***
Address: Faculty of Electrical Engineering, K. N. Toosi University of Technology, Seyed-Khandan Bridge, Shariati Ave., Tehran, Iran. Postal Code: 1631714191.
Phone: -
Fax: -
afnajafiafshin@gmail.com
m.vanak961@gmail.com

Article History
Received: June 26, 2026
Accepted: July 22, 2026
ePublished: September 01, 2026

ABSTRACT

Unit commitment (UC) is a key optimization problem in power system operation, but its computational burden increases rapidly when a system includes many identical or similar generating units. The aggregation of identical units can reduce this burden by replacing unit-level binary variables with aggregated integer variables. However, this simplification may reduce the accuracy of the obtained schedule because the operation of individual generating units is not fully represented. This paper proposes a tractable unit commitment (TUC) formulation to improve the computational performance of UC while preserving the accuracy of the unit-level solution. The proposed formulation connects the conventional UC model and the aggregated representation through linking constraints that enforce consistency between unit-level and aggregated variables. The model is tested on scaled IEEE 24-bus and IEEE 118-bus systems under different renewable penetration levels and battery energy storage scenarios. The results show that the aggregation-based formulation provides the shortest CPU time, but it underestimates the operating cost in all cases. In contrast, the proposed TUC formulation keeps the cost error almost equal to zero, with a maximum absolute error of 0.0009%, while reducing CPU time compared with UC. Additional comparisons of generation schedules, commitment decisions, and battery charging and discharging profiles show that TUC closely follows the UC benchmark. These results confirm that the proposed TUC formulation provides a better balance between computational efficiency and solution accuracy than the conventional aggregation-based formulation.

Keywords: Unit commitment; Unit aggregation; Tractable unit commitment; Linking constraints; Energy storage system; Renewable energy integration.

1 Introduction

Unit commitment (UC) is a central scheduling problem in power system operation. It determines the ON/OFF status, start-up and shut-down actions, and generation level of generating units over a short-term horizon. The objective is usually to minimize the total operating cost, including production cost, no-load cost, start-up and shut-down costs, reserve cost, and possible penalty costs, while satisfying demand balance, generation limits, ramping limits, minimum up-time and down-time constraints, reserve requirements, and network constraints [1], [2]. Since the commitment status of each generating unit is represented by binary variables and coupled across consecutive time periods, UC is commonly formulated as a mixed-integer optimization problem. Therefore, its computational burden can increase rapidly in large-scale systems with many units, long scheduling horizons, and detailed operational constraints. Several studies have improved UC formulations by developing tighter and more compact mixed-integer models, comparing alternative binary formulations, and analyzing the effect of formulation strength on computational performance [3-5]. Recent studies have continued to address the computational burden of UC from different perspectives. Efficient optimization methods have been reviewed for power systems with high renewable penetration, where large-scale and strongly coupled operational problems become more difficult to solve [6]. Other studies have proposed practical solution strategies for production-cost UC models, infeasibility cutting planes, and matheuristic approaches based on kernel search and local branching to reduce computational time [7]–[9]. In addition, learning-assisted UC methods have been developed to predict commitment decisions, warm start the solver, or incorporate machine-learning outputs while preserving feasibility [10], [11]. These recent works confirm that computational efficiency remains an active research topic in UC, especially when the problem includes many generating units, renewable generation, energy storage, or long operational horizons. This computational challenge becomes more serious when the system includes many identical or highly similar generating units. In such cases, several different ON/OFF combinations may represent the same physical operation and lead to the same objective value. This symmetry creates redundant solutions in the branch-and-bound search process and can increase CPU time without adding useful physical information to the schedule [12]. One group of studies has addressed this issue by using special branching rules or symmetry-breaking inequalities. These methods can remove part of the redundant search space and improve the solution process for highly symmetric UC instances. However, they do not fully eliminate all equivalent solutions, and symmetry-breaking inequalities may also increase the size of the LP relaxation. In addition, some branching-based approaches are not easy to implement in commercial solvers because they may require solver callbacks or may disable some advanced solver features [12]. Another group of studies has reduced the computational burden by using aggregated representations of similar or identical generating units. In these formulations, several unit-level binary commitment variables are replaced by integer variables that represent the number of committed, started-up, or shut-down units. This can significantly reduce the number of variables and the size of the commitment state space [13]. However, the aggregated representation may introduce approximation errors because it does not always preserve the operating trajectory of each individual unit. Previous studies have shown that aggregation may overestimate the flexibility of generating units, especially for start-up and shut-down capabilities, ramping limits, and minimum up-time and down-time constraints [13], [14]. In some cases, the aggregated solution may be infeasible when it is converted back to a unit-level schedule, because the aggregate generation level does not show how the output is distributed among individual units [13]. Several studies have attempted to reduce the gap between computational efficiency and unit-level accuracy in aggregated UC models. Koller and Hofmann [15] proposed a shifting generation level method to improve the clustering of identical generating units. Palmintier and Webster [16] developed a heterogeneous unit clustering approach for efficient operational flexibility modeling. Du et al. [17] proposed a network-constrained clustered UC model for power system planning studies. More recently, Zhang et al. [18] proposed a tight unit aggregation model to eliminate symmetry by adding tight constraints on the maximum aggregated power-output trajectory. Their study shows that aggregation can be strengthened to improve computational performance while preserving optimality under the assumptions of their formulation. However, aggregation-based approaches may still require additional variables, post-processing, special structural assumptions, or specific operating conditions to recover or guarantee individual-unit schedules. Due to their computational advantage, aggregated UC formulations have also been used in long-term operational and generation expansion planning studies. These models are especially useful when UC constraints must be embedded in planning problems with flexibility requirements and energy storage devices [19], [20]. This direction has become more important because high renewable penetration and energy storage integration increase the need for flexible scheduling models. Recent stochastic and storage-integrated planning studies have shown that renewable uncertainty, load variation, and storage operation can substantially increase the size and complexity of UC-based planning models [21], [22]. Therefore, tractable UC formulations that reduce computational burden without losing important unit-level operating information are increasingly needed. Although the above studies have improved the computational performance and accuracy of UC-based models, an important gap still remains. Symmetry-breaking methods can reduce part of the redundant search space, but they may not remove all equivalent solutions and may increase the model size. Aggregated UC formulations can reduce the number of binary variables, but they may lose exact unit-level operating information. Morales-España and Tejada-Arango [14] addressed part of this gap by adding individual-unit flexibility constraints to the CUC formulation. However, their model does not include the complete set of unit-level UC constraints, especially individual minimum up-time and down-time constraints, and therefore it cannot directly guarantee a complete exact unit-level feasible schedule. This indicates the need for a formulation that can improve computational performance while preserving the exactness of the unit-level UC solution. To address this limitation, this paper proposes a tractable unit commitment (TUC) formulation that connects the conventional UC and CUC formulations through linking constraints. The main idea is not to replace the unit-level UC model with an aggregated relaxation. Instead, the proposed formulation keeps the full set of unit-level UC constraints and simultaneously imposes aggregate-level consistency through linking constraints on commitment, generation, and reserve variables. These linking constraints force the aggregate variables to be consistent with the summation of the corresponding unit-level variables within each cluster. Therefore, they guide the branch-and-bound search by adding a structured aggregated representation while preserving the unit-level feasible region of the UC model. Since all original UC constraints are retained, every feasible solution of the proposed TUC model has an explicit unit-level commitment, start-up, shut-down, generation, and reserve schedule. Moreover, the linking constraints only enforce consistency between the unit-level variables and their aggregate counterparts. Therefore, the proposed model does not require a post-processing or disaggregation step to obtain the final unit-level schedule. This feature distinguishes the proposed formulation from conventional CUC models, where the aggregated solution may not directly represent a complete feasible schedule for individual units. The main contributions of this paper are summarized as follows:

- A tractable unit commitment (TUC) formulation is proposed by connecting the CUC and UC formulations through additional linking constraints. These constraints impose aggregate-level consistency on the unit-level variables, guide the branch-and-bound search, and reduce CPU time.
- Since all unit-level UC constraints are retained and all unit-level decision variables remain explicit, the proposed model provides an exact unit-level solution without requiring any post-processing or disaggregation step.
- The impacts of adding energy storage devices to the system and the accuracy of the CUC formulation are evaluated under different renewable penetration levels.

The rest of this paper is organized as follows. Section 2 presents the mathematical formulation of the proposed model. Section 3 describes the studied cases and input data. Section 4 presents and discusses the numerical results, including the computational performance, accuracy of the CUC formulation, and the impact of energy storage devices. Finally, Section 5 concludes the paper.

2 Mathematical Formulation

This section presents the mathematical formulation of the proposed tractable unit commitment (TUC) model. The index $t \in \Omega_T$ denotes the time period, $g \in \Omega_G$ denotes the individual generating unit, and $c \in \Omega_C$ denotes the generating-unit cluster. The set of generating units belonging to cluster c is denoted by Ω_G^c. Throughout the formulation, lowercase subscripts g, c, and t are used consistently for units, clusters, and time periods, respectively.

The symbols C_g^{VC}, C_g^{NL}, C_g^{SU}, and C_g^{R} denote the variable generation cost, no-load cost, start-up cost, and spinning reserve cost of generating unit g, respectively. Similarly, C_c^{VC}, C_c^{NL}, C_c^{SU}, and C_c^{R} denote the corresponding cost coefficients for cluster c. The parameter C^W denotes the wind curtailment cost coefficient, and C^B denotes the battery operating cost coefficient. The variables $p_{g,t}$, $u_{g,t}$, $v_{g,t}$, $w_{g,t}$, and $r_{g,t}^{+}$ represent the power output, commitment status, start-up status, shut-down status, and upward spinning reserve of unit g at time t, respectively. The corresponding cluster-level variables are denoted by $p_{c,t}$, $u_{c,t}$, $v_{c,t}$, $w_{c,t}$, and $R_{c,t}^{+}$. The variables P_t^{Curt}, $p_{dis,t}$, and $p_{ch,t}$ denote curtailed wind power, battery discharging power, and battery charging power at time t, respectively. For the UC formulation, the objective function is written based on unit-level variables as follows:

$$OC = \sum_{t=1}^{T}\Big[\sum_{g\in\Omega_G}(C_g^{VC}.p_{g,t} + C_g^{NL}.u_{g,t} + C_g^{SU}.v_{g,t} + C_g^{R}.r_{g,t}^{+}) + C^W.P_t^{Curt} + C^B(p_{dis,t} + p_{dis,t})\Big] \quad (1)$$

For the CUC and TUC formulations, the equivalent objective function is expressed using cluster-level variables as follows:

$$OC = \sum_{t=1}^{T}\Big[\sum_{c\in\Omega_C}(C_c^{VC}.p_{c,t} + C_c^{NL}.u_{c,t} + C_c^{SU}.v_{c,t} + C_c^{R}.R_{c,t}^{+}) + C^W.P_t^{Curt} + C^B(p_{dis,t} + p_{dis,t})\Big] \quad (2)$$

The domains of the decision variables are defined as follows. The unit-level commitment, start-up, and shut-down variables are binary variables: $u_{g,t}, v_{g,t}, w_{g,t} \in \{0,1\}\ \forall\ g \in \Omega_G, \forall\ t \in \Omega_T$. The cluster-level commitment, start-up, and shut-down variables are non-negative integer variables: $u_{c,t}, v_{c,t}, w_{c,t} \in Z^{+}, \forall\ c \in \Omega_C, \forall\ t \in \Omega_T$. The charging/discharging mode variable of the energy storage system is also binary: $b_t \in \{0,1\}, \forall\ t \in \Omega_T$. All generation, reserve, wind curtailment, battery charging/discharging power, and stored energy variables are continuous variables: $p_{g,t}$, $p_{g,t}{}^{*}$, $r_{g,t}^{+}$, $p_{c,t}$, $p_{c,t}{}^{*}$, $R_{c,t}^{+}$, P_t^{Curt}, $p_{ch,t}$, $p_{dis,t}$, $e_t \in R^{+}, \forall\ g \in \Omega_G, \forall\ c \in \Omega_C, \forall\ t \in \Omega_T$. Therefore, the proposed formulation is a mixed-integer linear programming model, including binary unit-level variables, integer cluster-level variables, and continuous operational variables. The constraints of the model are presented in the following subsections. The first part provides the UC constraints, which are given in Eqs. (3)-(14).

2.1 UC Constraints

The logical constraints of the UC formulation are presented in Eqs. (3) and (4). Eq. (3) defines the relationship between the commitment status, start-up variable, and shut-down variable of each generating unit. According to this equation, a change in the commitment status between two consecutive time periods is represented by either a start-up or a shut-down action. Eq. (4) prevents a generating unit from being started up and shut down at the same time. Unless otherwise stated, all constraints presented hereafter are imposed for all time periods, generating units, and generating-unit clusters.

$$u_{g,t} - u_{g,t-1} = v_{g,t} - w_{g,t} \tag{3}$$

$$v_{g,t} + w_{g,t} \leq 1 \tag{4}$$

Eqs. (5) and (6) enforce the minimum up-time and minimum down-time constraints of generating units, respectively. Eq. (5) ensures that if unit g is started up, it must remain online for at least MUT_g consecutive time periods. Similarly, Eq. (6) guarantees that if unit g is shut down, it must remain offline for at least MDT_g consecutive time periods.

$$\sum_{\tau=t-MUT_g+1}^{t} v_{g,\tau} \leq u_{g,t} \tag{5}$$

$$\sum_{\tau=t-MDT_g+1}^{t} w_{g,\tau} \leq 1 - u_{g,t} \tag{6}$$

Eqs. (7)-(9) impose the upper generation and upward reserve limits of generating units by considering their start-up and shut-down capabilities. In these constraints, $p_{g,t}{}^*$ denotes the power output of unit g above its minimum generation level. The terms SU_g and SD_g denote the start-up and shut-down capabilities of unit g, respectively.

Eqs. (7) and (8) are applied to generating units with (MUT_g=1). For these units, start-up and shut-down actions may occur in consecutive time periods, and therefore both start-up and shut-down capabilities must be explicitly considered in limiting the available generation and upward reserve. Eq. (7) limits the output and reserve when the future shut-down action is binding, while Eq. (8) limits them when the current start-up action is binding.

Eq. (9) is applied to generating units with (MUT_g>1). Since these units must remain online for more than one time period after start-up, simultaneous or consecutive start-up and shut-down effects are more restricted. Therefore, a single upper-bound constraint is used to limit the available generation and upward reserve during start-up and shut-down periods.

$$p_{g,t}{}^* + r_{g,t}^+ \leq (P_g^{max} - P_g^{min}).u_{g,t} - (P_g^{max} - SD_g).w_{g,t+1} \tag{7}$$

$$p_{g,t}{}^* + r_{g,t}^+ \leq (P_g^{max} - P_g^{min}).u_{g,t} - (P_g^{max} - SU_g).v_{g,t} \tag{8}$$

$$p_{g,t}{}^* + r_{g,t}^+ \leq (P_g^{max} - P_g^{min}).u_{g,t} - (P_g^{max} - SU_g).v_{g,t} - (P_g^{max} - SD_g).w_{g,t+1} \tag{9}$$

Eq. (10) enforces the non-negativity of $p_{g,t}{}^*$, which represents the power output of unit g above its minimum generation level. Eq. (11) defines the total power output of unit g as the sum of $p_{g,t}{}^*$ and the minimum generation level when the unit is online.

$$p_{g,t}{}^* \geq 0 \tag{10}$$

$$p_{g,t} = p_{g,t}{}^* + u_{g,t}.P_g^{min} \tag{11}$$

Eqs. (12) and (13) represent the ramp-up and ramp-down constraints of generating units, respectively. Eq. (12) limits the increase in the power output above the minimum generation level between two consecutive time periods, while also considering the upward reserve scheduled at time t. The right-hand side of this constraint accounts for the ramp-up capability RU_g and the start-up capability SU_g of unit g. Eq. (13) limits the decrease in the power output above the minimum generation level between two consecutive time periods by considering the ramp-down capability RD_g and the shut-down capability SD_g. These constraints are applied for $t \neq 1$, since they require the power output of the previous time period.

$$p_{g,t}{}^* + r_{g,t}^+ - p_{g,t-1}{}^* \leq RU_g.u_{g,t} + v_{g,t}.\left(SU_g - P_g^{min} - RU_g\right) \tag{12}$$

$$p_{g,t-1}{}^* - p_{g,t}{}^* \leq RD_g.u_{g,t-1} + w_{g,t}.\left(SD_g - P_g^{min} - RD_g\right) \tag{13}$$

Eq. (14) defines the spinning reserve requirement of the system. This constraint ensures that the total upward reserve provided by generating units is not less than the required spinning reserve at time t.

$$\sum_{g\in\Omega_G} r_{g,t}^+ \geq RT_t \tag{14}$$

The second part of the formulation presents the CUC constraints, which are given in Eqs. (15)-(26).

2.2 Clustered UC Constraints

Eqs. (15)-(18) represent the cluster-level counterparts of the UC logical and minimum up/down-time constraints. In these equations, the unit index g is replaced by the cluster index c, and the binary commitment, start-up, and shut-down variables are replaced by integer variables that indicate the number of committed, started-up, and shut-down units in cluster c. The parameter N_C denotes the number of generating units in cluster c.

$$u_{c,t} - u_{c,t-1} = v_{c,t} - w_{c,t} \tag{15}$$

$$u_{c,t} \leq N_c \tag{16}$$

$$\sum_{\tau=t-MUT_c+1}^{t} v_{c,\tau} \leq u_{c,t} \tag{17}$$

$$\sum_{\tau=t-MDT_c+1}^{t} w_{c,\tau} \leq N_c - u_{c,t} \tag{18}$$

Eqs. (19)-(23) define the generation output limits of the CUC formulation. These constraints are the cluster-level counterparts of the corresponding UC constraints. In these equations, $p_{c,t}{}^*$ denotes the aggregated power output above the minimum generation level of cluster c, and $R_{c,t}^+$ represents the upward reserve provided by cluster c at time t. Parameters P_c^{max} and P_c^{min} denote the maximum and minimum power output of the units represented by cluster c, while SU_c and SD_c represent their start-up and shut-down capabilities, respectively.

$$p_{c,t}{}^* + R_{c,t}^+ \leq (P_c^{max} - P_c^{min}).u_{c,t} - (P_c^{max} - SD_c).w_{c,t+1} \tag{19}$$

$$p_{c,t}{}^* + R_{c,t}^+ \leq (P_c^{max} - P_c^{min}).u_{c,t} - (P_c^{max} - SU_c).v_{c,t} \tag{20}$$

$$p_{c,t}{}^* + R_{c,t}^+ \leq \left(P_c^{max} - P_c^{min}\right).u_{c,t} - (P_c^{max} - SU_c).v_{c,t} - (P_c^{max} - SD_c).w_{c,t+1} \tag{21}$$

$$p_{c,t}{}^* \geq 0 \tag{22}$$

$$p_{c,t} = p_{c,t}{}^* + u_{c,t}.P_c^{min} \tag{23}$$

Eqs. (24) and (25) represent the cluster-level ramp-up and ramp-down constraints, respectively. Eq. (24) limits the increase in the aggregated power output above the minimum generation level between two consecutive time periods, while also considering the upward reserve scheduled for cluster c at time t. The right-hand side of this constraint accounts for the ramp-up capability RU_c of the committed units and the start-up capability SU_c of the units that are started up at time t. Eq. (25) limits the decrease in the aggregated power output above the minimum generation level between two consecutive time periods by considering the ramp-down capability RD_c and the shut-down capability SD_c. These constraints are applied for $t \neq 1$, since they depend on the power output of the previous time period.

$$p_{c,t}{}^{*} - p_{c,t-1}{}^{*} + R_{c,t}^{+} \leq RU_c.\left(u_{c,t} - v_{c,t}\right) + v_{c,t}.\left(SU_c - P_c^{min}\right) \quad (24)$$

$$p_{c,t-1}{}^{*} - p_{c,t}{}^{*} \leq RD_c.\left(u_{c,t-1} - w_{c,t}\right) + w_{c,t}.\left(SD_c - P_c^{min}\right) \quad (25)$$

Eq. (26) defines the spinning reserve requirement in the CUC formulation. This constraint ensures that the total upward reserve provided by all generating-unit clusters is not less than the required spinning reserve at time t.

$$\sum_{c \in \Omega_C} R_{c,t}^{+} \geq RT_t \quad (26)$$

The third part of the formulation presents the linking constraints of the proposed TUC model, which are given in Eqs. (27)-(29).

2.3 Linking Constraints

These constraints connect the cluster-level variables of the CUC formulation with the unit-level variables of the UC formulation.

Eq. (27) defines the upward reserve of cluster c as the summation of the upward reserves provided by all generating units within that cluster. Eq. (28) links the total power output of cluster c to the sum of the power outputs of its individual generating units. Eq. (29) ensures that the number of committed units in cluster c is equal to the summation of the commitment statuses of the individual units belonging to that cluster. These linking constraints allow the proposed TUC formulation to connect the aggregated CUC representation with the unit-level UC formulation.

$$R_{c,t}^{+} = \sum_{g \in \Omega_G^c} r_{g,t}^{+} \quad (27)$$

$$p_{c,t} = \sum_{g \in \Omega_G^c} p_{g,t} \quad (28)$$

$$u_{c,t} = \sum_{g \in \Omega_G^c} u_{g,t} \quad (29)$$

Remark 1. Exactness of the proposed TUC formulation: Let F_UC denote the feasible set of the unit-level UC formulation defined by Eqs. (3)–(14) together with the system and ESS constraints. In the proposed TUC formulation, all constraints of the unit-level UC model are retained. Therefore, any feasible solution of the TUC model directly satisfies all unit-level logical, minimum up/down-time, generation-limit, ramping, reserve, and storage constraints. In addition, the linking constraints in Eqs. (27)–(29) only enforce consistency between the aggregate variables and the corresponding summation of the unit-level variables. Hence, the proposed TUC formulation does not rely on an approximate disaggregation of the cluster-level solution. The commitment, start-up, shut-down, generation, and reserve schedules of individual units are explicitly obtained from the optimization model. Therefore, the proposed formulation provides an exact unit-level solution without requiring any post-processing step.

2.4 System Constraints

System-level constraints are presented in Eqs. (30) and (31). Eq. (30) calculates the spinning reserve requirement at time t. The required reserve is determined as a fraction of the load demand D_t and the net wind power after curtailment ($PW_t - P_t^C$), where γ_1 and γ_2 are the reserve requirement coefficients. Eq. (31) represents the system power balance constraint. This equation ensures that the total power generated by thermal units, the net wind power after curtailment, and the battery discharging power are equal to the load demand plus the battery charging power at each time period. In this equation, $p_{dis,t}$ and $p_{ch,t}$ denote the battery discharging and charging power at time t, respectively.

It should be noted that Eq. (31) represents a system-level power balance constraint. Therefore, the scheduling problem is modeled as a single-bus equivalent system, in which all thermal generation, wind generation, battery energy storage, and load demand are aggregated at the system level. Transmission network constraints, including bus voltage angles, line-flow equations, and transmission capacity limits, are not explicitly considered in the present formulation. This modeling choice is adopted because the main purpose of this paper is to evaluate the computational performance and unit-level accuracy of aggregation-based UC formulations for systems with many identical generating units, rather than to study network congestion or locational effects. This focus is consistent with aggregation-oriented UC studies that investigate the computational effects of identical generating units and aggregated commitment representations [12], [18].

$$RT_t = \gamma_1.D_t + \gamma_2\left(PW_t - P_t^{Curt}\right) \quad (30)$$

$$\sum_{g \in \Omega_G} p_{g,t} + PW_t - P_t^{Curt} + p_{dis,t} - p_{ch,t} = D_t \quad (31)$$

2.5 Energy Storage Constraints

The energy storage system constraints are adapted from the BES modeling approach used in [20]. Energy storage system constraints are presented in Eqs. (32)-(37). Eq. (32) describes the energy balance of the battery. In this equation, e_t denotes the stored energy in the battery at time t, B_{sd} is the self-discharge rate, α represents the battery efficiency, and $p_{ch,t}$ and $p_{dis,t}$ denote the battery charging and discharging power at time t, respectively. Eq. (33) imposes the initial and final energy levels of the battery, where DOD is the depth of discharge and $Emax$ is the maximum energy capacity of the battery. Eq. (34) defines the maximum energy capacity of the battery based on the energy-to-power ratio EPR and the maximum battery power $Pmax$.

Eqs. (35) and (36) limit the charging and discharging power of the battery, respectively. In these equations, b_t is a binary variable used to prevent simultaneous charging and discharging. When $b_t = 1$, the battery can be charged, while discharging is not allowed. When $b_t = 0$, the battery can be discharged, while charging is not allowed. Eq. (37) limits the stored energy of the battery between its minimum allowable level and maximum energy capacity.

Table 1: Constraint sets used in the studied formulations

Constraint group	UC	CUC	TUC
Objective function	Eq. (1)	Eq. (2)	
UC constraints	Eqs. (3)-(14)	-	Eqs. (3)-(14)
CUC constraints	-	Eqs. (15)-(26)	
Linking constraints	-		Eqs. (27)-(29)
System constraints	Eqs. (30)-(31)		
ESS constraints	Eqs. (32)-(37)		

$$e_t = (1 - B_{sd}).e_{t-1} + \alpha.p_{ch,t} - \frac{1}{\alpha}.p_{dis,t} \quad (32)$$

$$e_0 = e_{24} = (1 - DOD).Emax \quad (33)$$

$$Emax = EPR * Pmax \quad (34)$$

$$p_{ch,t} \leq b_t Pmax \quad (35)$$

$$p_{dis,t} \leq (1 - b_t)Pmax \quad (36)$$

$$(1 - DOD)Emax < e_t < Emax \quad (37)$$

3 Case Studies and Input Data

This section presents the studied formulations, test systems, input data, and simulation cases used to evaluate the performance of the proposed TUC model. First, the implemented UC-based formulations are summarized to clarify the set of constraints used in each model. Then, the test systems, generating unit data, load and wind profiles, energy storage parameters, simulation scenarios, and performance criteria are described.

3.1 Studied Formulations

Three UC-based formulations are implemented and compared in this study: the conventional UC model, the CUC model, and the proposed TUC model. The UC model is formulated at the unit level and is used as the reference model. The CUC model represents similar generating units at the cluster level to reduce the number of binary variables. The proposed TUC model connects the UC and CUC formulations through the linking constraints. Table 1 summarizes the constraint sets used in each formulation.

As shown in Table 1, the proposed TUC formulation differs from the conventional UC and CUC models by simultaneously including the UC and CUC constraints and connecting them through the linking constraints. This structure is used to improve the computational performance while preserving the unit-level representation of the UC solution. Compared with the conventional UC formulation, the proposed TUC formulation does not remove the unit-level binary variables. Instead, it augments the unit-level UC model with aggregate CUC variables and aggregate-level constraints. The linking constraints make the aggregate commitment, generation, and reserve variables consistent with the corresponding summation of unit-level variables. Therefore, during the branch-and-bound process, the solver is guided not only by individual unit-level decisions, but also by cluster-level bounds on commitment, generation, ramping capability, and reserve. This additional aggregate structure tightens the search process and reduces redundant exploration among identical generating units, while the unit-level UC variables and constraints are still retained.

3.2 Test Systems and Input Data

Two IEEE benchmark systems are used in this study to construct the generation and load data of the studied UC instances: the IEEE 24-bus system and the IEEE 118-bus system. The complete input data, including generating-unit data, hourly load demand, and hourly wind power profile, are available in [23]. The original IEEE 24-bus system includes 24 buses, 38 transmission lines, and a peak demand of 2850 MW. Similar to [5], the number of generating units and the load demand of the standard test systems are scaled by a factor of 10 in order to create larger UC instances with many identical generating units. Therefore, the scaled IEEE 24-bus system includes 360 generating units and a scaled peak demand of 28500 MW, while the scaled IEEE 118-bus system includes 540 generating units. The generating units are grouped according to their technical and economic characteristics, such as minimum and maximum generation limits, ramp-up and ramp-down limits, start-up and shut-down capabilities, minimum up-time and down-time, and cost coefficients. In the present study, the scaled IEEE test systems are constructed by replicating the original generating units. Therefore, the replicated units obtained from the same original unit are treated as identical units and are assigned to the same cluster. For each cluster c, Nc denotes the number of identical generating units in that cluster. The technical and economic parameters of each cluster are taken from the corresponding representative unit. In the present study, the IEEE systems are represented using a single-bus equivalent framework. Therefore, the thermal generating units, wind generation, battery energy storage, and load demand are aggregated at the system level. Due to this modeling assumption, the bus-by-bus network topology, the exact location of resources, nodal power balance constraints, line-flow equations, bus voltage angles, and transmission capacity limits are not explicitly modeled in the optimization problem. The hourly wind power profile is provided in the online repository [23] and scaled to obtain the considered renewable penetration levels. In this study, the 25% and 50% renewable penetration levels mean that the total available wind energy over the 24-hour scheduling horizon is equal to 25% and 50% of the total load energy over the same horizon, respectively. In addition, large-scale battery energy storage is included in Scenarios 3 and 4 to evaluate the effect of storage flexibility on the accuracy and computational performance of the studied formulations. The battery efficiency is set to 87%, the self-discharge rate is assumed to be zero, the depth of discharge is set to 0.8, and the energy-to-power ratio is set to 12 h. The maximum aggregated energy capacity of the battery energy storage system is 18 GWh for the IEEE 24-bus test system and 36 GWh for the IEEE 118-bus test system. Accordingly, the corresponding maximum charging/discharging power ratings are 1.5 GW and 3 GW, respectively. The battery operating cost coefficient is set to 5 $/MWh for the IEEE 24-bus test system and 10 $/MWh for the IEEE 118-bus test system. The wind curtailment cost is set to

500 \$/MW, and the reserve requirement coefficients are set to $\gamma_1 = 0.03$ and $\gamma_2 = 0.05$.

3.3 Simulation Scenarios

Four operating scenarios are considered for each test system. In Scenario 1, the renewable energy penetration level is 25%. In Scenario 2, the renewable energy penetration level is 50%. Scenarios 3 and 4 correspond to Scenarios 1 and 2, respectively, with the inclusion of large-scale battery energy storage systems. The 25% renewable penetration level means that the total wind energy over the 24-hour horizon is equal to 25% of the total load energy over the same horizon. Similarly, the 50% renewable penetration level means that the total wind energy over the 24-hour horizon is equal to 50% of the total load energy. The 24-hour load demand and wind power profile of the IEEE 24-bus system under 50% renewable penetration are shown in Figure 1.

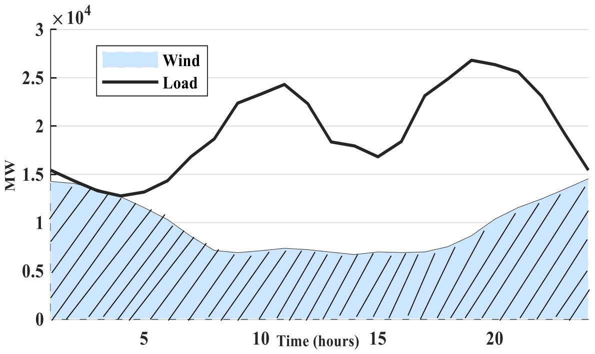

Figure 1: Hourly load demand and wind power profile of the IEEE 24-bus system under 50% renewable penetration.

Both test systems are simulated under the four operating scenarios. Therefore, eight simulation cases are considered in total. Cases 1–4 correspond to the IEEE 24-bus system under Scenarios 1–4, respectively. Cases 5–8 correspond to the IEEE 118-bus system under Scenarios 1–4, respectively.

3.4 Simulation Settings and Performance Criteria

All simulations are implemented in GAMS and solved using the Gurobi 8 solver on a PC with an Intel Core i7-11800H CPU at 4.2 GHz and 16 GB RAM. The optimality gap is set to 0.02% for all cases.
To compare the performance of the studied formulations, two criteria are used: the relative objective function error and the CPU time. The conventional UC formulation is considered as the benchmark. The relative objective function error of each formulation with respect to the UC solution is calculated as follows:

$$e^{cost} = \frac{(C^{TOT} - \bar{C}^{TOT})}{\bar{C}^{TOT}} \tag{38}$$

where C^{TOT} is the total operating cost obtained by the studied formulation, and $\bar{C}^{TOT}$ is the total operating cost obtained by the UC benchmark. A lower value of e^{cost} indicates a smaller deviation from the UC benchmark. The CPU time is also reported to evaluate the computational performance of each formulation. In addition, the speed-up factor is used to provide a normalized comparison of the computational performance of the studied formulations. The speed-up factor of formulation m is calculated with respect to the conventional UC formulation based on Eq. (39):

$$Speed - up - factor^{m} = \frac{CPUTime^{UC}}{CPUTime^{m}} \tag{39}$$

4 Numerical Results and Discussion

The simulation results are reported in Table 2. This table compares the performance of the UC, CUC, and TUC formulations in terms of cost error, CPU time, and speed-up factor for the IEEE 24-bus and IEEE 118-bus systems. The speed-up factor is calculated based on Eq. (39), where the CPU time of the conventional UC formulation is used as the benchmark in each case. The results show that both the CUC and TUC formulations reduce the CPU time compared with the conventional UC formulation. The CUC formulation achieves the lowest CPU time in all cases because it represents similar generating units at the cluster level and reduces the number of binary variables. However, this computational advantage is obtained with a noticeable deviation from the UC benchmark. The negative cost errors of the CUC formulation in all cases show that CUC underestimates the operating cost compared with UC.
The impact of renewable penetration and ESS on the accuracy of the CUC formulation can be observed by comparing the absolute cost errors reported in Table 2. In most cases, increasing the renewable penetration from 25% to 50% increases the absolute cost error of CUC. This trend is observed in three out of the four corresponding comparisons. For example, in the IEEE 118-bus system without ESS, the absolute CUC cost error increases from 0.1296% to 0.7381% when the renewable penetration increases from 25% to 50%. A similar increase is also observed in both test systems when ESS is included. The only exception is the IEEE 24-bus system without ESS, where the absolute CUC cost error decreases from 0.2526% to 0.2048%. Therefore, higher renewable penetration generally makes the approximation error of CUC more significant. The effect of ESS on the CUC accuracy is also shown in Table 2. In three out of the four corresponding comparisons, adding ESS reduces the absolute CUC cost error. In the IEEE 24-bus system with 25% renewable penetration, the absolute CUC cost error decreases from 0.2526% to 0.1931% after adding ESS. In the IEEE 118-bus system, adding ESS reduces the absolute CUC cost error from 0.1296% to 0.0875% under the 25% renewable scenario and from 0.7381% to 0.5730% under the 50% renewable scenario. The only exception is the IEEE 24-bus system with 50% renewable penetration, where the absolute CUC cost error increases from 0.2048% to 0.3017% after adding ESS. Therefore, although the effect of ESS is not completely uniform, ESS reduces the approximation error of CUC in most cases by providing additional operational flexibility.
In contrast, the proposed TUC formulation keeps the cost error almost equal to zero in all cases. The maximum absolute cost error of TUC is only 0.0008%, which confirms that the

proposed formulation preserves the unit-level accuracy of the UC benchmark. At the same time, TUC reduces the CPU time compared with UC in all cases. According to the speed-up factors reported in Table 2, the TUC formulation achieves speed-up factors of 2.6, 5.55, 1.2, and 24 in the four IEEE 24-bus cases, respectively. For the IEEE 118-bus system, the corresponding speed-up factors are 1.6, 4.03, 1.5, and 1.45, respectively. The highest speed-up of the proposed TUC formulation is obtained in the IEEE 24-bus system with 50% renewable penetration and ESS, where the CPU time is reduced from 1755 s in UC to 73 s in TUC. In the IEEE 118-bus system, the highest TUC speed-up is obtained under the 50% renewable scenario without ESS, where the CPU time is reduced from 2095 s in UC to 519 s in TUC. Although CUC gives higher speed-up factors, it also introduces noticeable cost errors. Therefore, the proposed TUC formulation provides a better compromise between computational efficiency and solution accuracy.

To further evaluate the accuracy of the generation scheduling results, the normalized cluster-level generation outputs of the TUC and CUC formulations are compared with the UC benchmark. The overbar in $\bar{p}_{c,t}$ denotes the generation output obtained from the UC formulation. Therefore, the ratios ${P_{c,t}}^{TUC}/\bar{p}_{c,t}$ and ${P_{c,t}}^{CUC}/\bar{p}_{c,t}$ measure the deviation of the TUC and CUC generation schedules from the UC benchmark, respectively. Figure 2 compares ${P_{c,t}}^{TUC}/\bar{p}_{c,t}$ and ${P_{c,t}}^{CUC}/\bar{p}_{c,t}$ for all clusters at hour 10 in Case 6. Figure 3 compares the same ratios for cluster 11 over the 24-hour scheduling horizon in Case 6. In these figures, a value located on the circle with radius 1 indicates that the corresponding formulation gives the same generation output as the UC benchmark. Values greater than 1 show overestimation of the generation output, while values lower than 1 show underestimation. Further insight into the differences among the studied formulations can be obtained by comparing the commitment schedules and battery operating schedules. Figure 4 shows the number of committed units in cluster 18 over the 24-hour horizon for Case 2. It can be observed that the commitment schedule obtained by the proposed TUC formulation is identical to that of the UC benchmark in all hours. In contrast, the CUC formulation gives a different number of committed units in several hours.

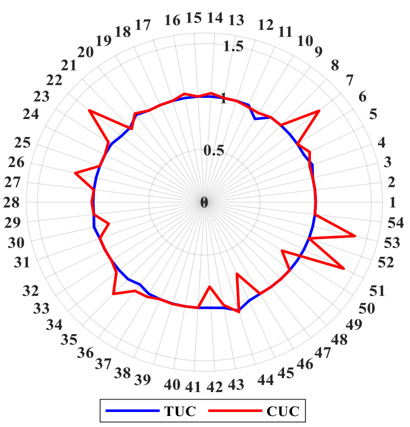

Figure 2: Normalized cluster-level generation output of the CUC and TUC formulations compared with the UC benchmark for all clusters at hour 10 in Case 6.

Table 2: Comparison of cost error, CPU time, and speed-up factor for the UC, CUC, and TUC formulations under different renewable penetration and ESS scenarios in the scaled IEEE 24-bus and IEEE 118-bus systems.

Case	Error metrics	IEEE-24 bus			IEEE-118 bus		
		360-gen			540-gen		
		UC	CUC	TUC	UC	CUC	TUC
25% Renewable	Cost error [%]	-	-0.2526	**0.0001**	-	-0.1296	**-0.0003**
	CPU time [s]	217	1	81	218	1.5	134
	Speed-up factor	1	217	2.6	1	145	1.6
50% Renewable	Cost error [%]	-	-0.2048	**0.0000**	-	-0.7381	**0.0001**
	CPU time [s]	772	3	139	2095	21	519
	Speed-up factor	1	257	5.55	1	100	4.03
25% Renewable +ESS	Cost error [%]	-	-0.1931	**-0.000**	-	-0.0875	**-0.0000**
	CPU time [s]	13	0.7	11	24	1	16
	Speed-up factor	1	18.5	1.2	1	24	1.5
50% Renewable +ESS	Cost error [%]	-	-0.3017	**0.0000**	-	-0.5730	**-0.0008**
	CPU time [s]	1755	1	73	587	5	404
	Speed-up factor	1	1755	24	1	117.5	1.45

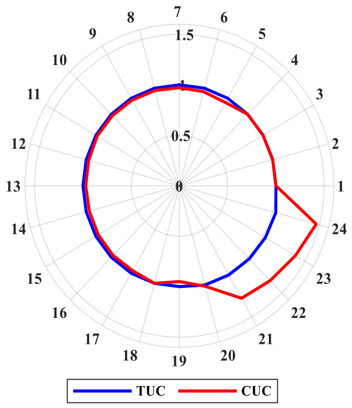

Figure 3: Normalized generation output of cluster 11 over the 24-hour scheduling horizon in Case 6, using the UC solution as the benchmark.

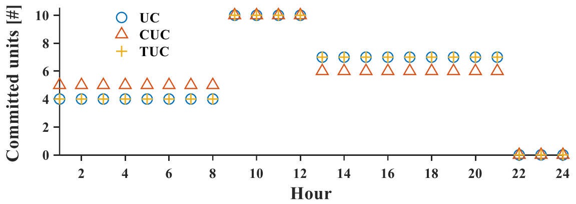

Figure 4: Number of committed units in cluster 18 over the 24-hour scheduling horizon in Case 2 obtained by the UC, CUC, and TUC formulations.

Figure 5 compares the charging and discharging power schedules obtained by the UC, CUC, and TUC formulations in Case 8. The charging power is plotted downward only for visual separation, while its axis labels are shown as positive values. The results show that, when battery energy storage systems are included in the unit commitment study, the CUC formulation may schedule the battery charging and discharging power inaccurately. In contrast, the proposed TUC formulation follows the UC benchmark very closely, with only negligible deviation. This result further confirms that the proposed linking constraints allow the TUC formulation to preserve the accuracy of the UC solution not only in generation scheduling, but also in the scheduling of energy storage operation.

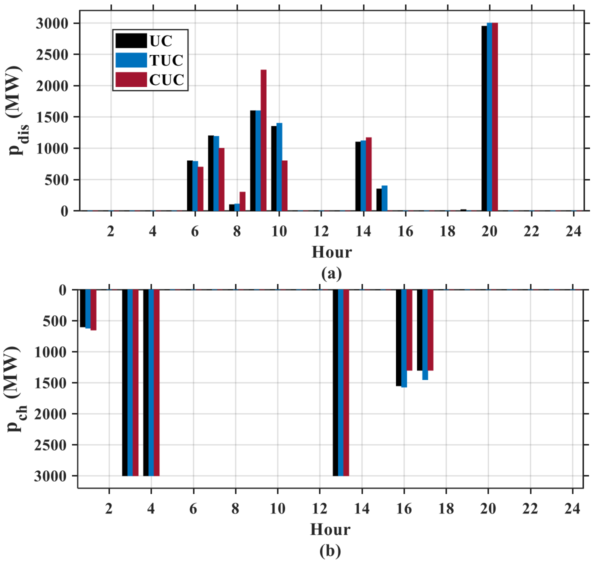

Figure 5: Battery power schedules obtained by the UC, CUC, and TUC formulations in Case 8: (a) discharging power $p_{dis,t}$, and (b) charging power $p_{ch,t}$.

4.1 Sensitivity Analysis on ESS Energy Capacity

To further evaluate the effect of storage capacity on the accuracy of the studied formulations, a sensitivity analysis is performed by varying the ESS energy capacity under the 50% renewable penetration scenario. Figures 6 and 7 show the absolute cost error of the CUC and TUC formulations for different ESS energy capacities in the IEEE 24-bus and IEEE 118-bus systems, respectively. As shown in Figure 6, in the IEEE 24-bus system, the absolute cost error of the CUC formulation first decreases as the ESS energy capacity increases. More specifically, the error decreases from 0.2048% at 0 GWh to 0.1450% at 12 GWh. This shows that adding storage can reduce the approximation error of CUC over a certain capacity range. However, the error does not change monotonically for larger ESS capacities. It increases to 0.3017% at 18 GWh and then remains higher than its minimum value at 21 GWh and 24 GWh. Therefore, the comparison between only the no-storage case and the base-storage case may suggest that ESS increases the CUC error, while the extended sensitivity analysis shows that the effect of ESS capacity is more complex and depends on the storage size. Figure 7 presents the corresponding results for the IEEE 118-bus system. In this case, the absolute cost error of the CUC formulation decreases steadily as the ESS energy capacity increases. The error decreases from 0.7381% at 0 GWh to 0.4630% at 48 GWh. This indicates that, in the larger test system, increasing the ESS energy capacity can mitigate the cost deviation of the CUC formulation from the UC benchmark. Nevertheless, even at the highest tested ESS capacity, the CUC formulation still has a noticeable error compared with the UC solution. In contrast, the proposed TUC formulation keeps the absolute cost error almost equal to zero for all tested ESS energy capacities in both test systems. In the IEEE 24-bus system, the maximum absolute cost error of TUC is only 0.0009%. In the IEEE 118-bus system, the maximum absolute cost error of TUC is only 0.0008%. These results confirm that the proposed TUC formulation preserves the unit-level accuracy of the UC benchmark under different storage capacity levels, while the accuracy of the CUC formulation is more sensitive to the ESS capacity and system size.

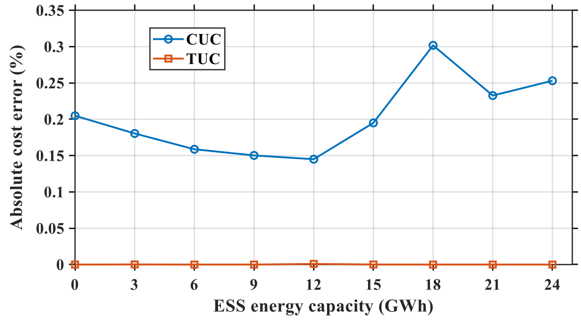

Figure 6: Effect of ESS energy capacity on the absolute cost error of the CUC and TUC formulations in the IEEE 24-bus system under 50% renewable penetration.

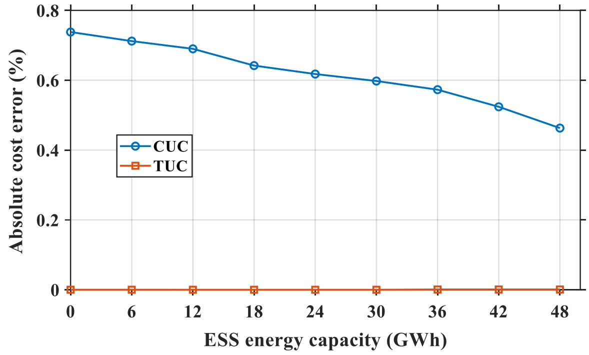

Figure 7: Effect of ESS energy capacity on the absolute cost error of the CUC and TUC formulations in the IEEE 118-bus system under 50% renewable penetration.

4.2 Sensitivity Analysis on Renewable Penetration

To further examine the impact of renewable penetration on the accuracy of the studied formulations, an additional sensitivity analysis is performed for the IEEE 24-bus system with ESS. In this analysis, the renewable penetration level is varied from 0% to 50%, while the ESS parameters are kept fixed. Figure 8 compares the absolute cost error of the CUC and TUC formulations under different renewable penetration levels. As shown in Figure 8, the absolute cost error of the CUC formulation increases as the renewable penetration level increases. The error increases from 0.0200% at 0% renewable penetration to 0.0570% at 10%, 0.1931% at 25%, 0.2300% at 40%, and 0.3017% at 50%. This result shows that, even in the presence of ESS, higher renewable penetration makes the approximation error of the CUC formulation more significant. This observation is also consistent with the findings reported in [13], where the accuracy of clustered unit commitment was shown to be affected by the operating conditions and system flexibility requirements. This behavior can be explained by the fact that higher renewable penetration increases the variability of net load and makes the scheduling problem more dependent on unit-level commitment, ramping, and flexibility constraints. In contrast, the proposed TUC formulation keeps the absolute cost error almost equal to zero for all tested renewable penetration levels. The maximum absolute cost error of TUC in this sensitivity analysis is only 0.0002%. This confirms that the proposed TUC formulation preserves the unit-level accuracy of the UC benchmark even when renewable penetration increases in the presence of ESS.

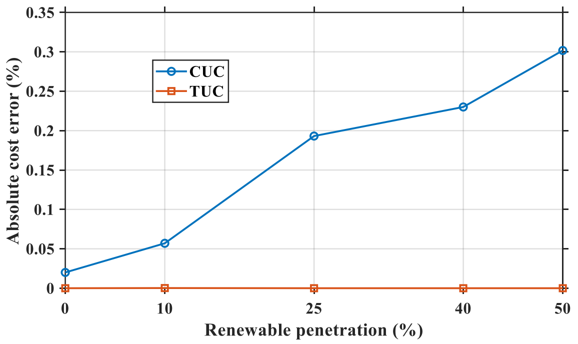

Figure 8: Effect of renewable penetration on the absolute cost error of the CUC and TUC formulations in the IEEE 24-bus system with ESS.

5 Conclusion

This paper proposed a tractable unit commitment (TUC) formulation to reduce the computational burden of UC problems with many similar generating units. The proposed formulation connects the UC and CUC models through linking constraints. In this way, it benefits from the compact structure of CUC while preserving the unit-level accuracy of UC. The proposed model was tested on scaled IEEE 24-bus and IEEE 118-bus systems under different renewable penetration levels and energy storage scenarios. The results showed that CUC gives the lowest CPU time, but it may underestimate the operating cost and produce inaccurate generation, commitment, and storage schedules. In contrast, TUC kept the cost error almost equal to zero in the main simulation cases, with a maximum absolute error of 0.0008%, while reducing the CPU time compared with UC. Additional sensitivity analyses were also performed to evaluate the effects of ESS energy capacity and renewable penetration. The results showed that the accuracy of the CUC formulation is sensitive to the ESS capacity, renewable penetration level, and system size. In the IEEE 24-bus system, increasing the ESS capacity reduced the CUC error only up to a certain range, while in the IEEE 118-bus system, the CUC error decreased more steadily as the ESS capacity increased. Moreover, increasing renewable penetration increased the CUC approximation error in the IEEE 24-bus system with ESS. In contrast, the proposed TUC formulation maintained an almost zero cost error in all sensitivity cases, with the maximum absolute error remaining below 0.001%. The numerical results confirm that TUC provides a better balance between computational efficiency and solution accuracy than CUC. Therefore, the proposed formulation can be used as a reliable alternative for large-scale UC studies with similar generating units, renewable generation, and energy storage systems. Future work can extend the proposed TUC formulation to stochastic or robust UC frameworks in order to consider uncertain load demand, renewable generation, and electricity prices.

6 Acknowledgement

Not applicable.

Disclosure of Potential Conflicts of Interest

The authors declare that there is no conflict of interest.

Reference

[1] Padhy NP. Unit Commitment: A Bibliographical Survey. IEEE Transactions on Power Systems 2004 May;19(2):1196-1205. doi: 10.1109/TPWRS.2003.821611.
[2] Carrión M and Arroyo JM. A Computationally Efficient Mixed-Integer Linear Formulation for the Thermal Unit Commitment Problem. IEEE Transactions on Power Systems 2006 Aug;21(3):1371-1378. doi: 10.1109/TPWRS.2006.876672.
[3] Morales-España G, Latorre JM and Ramos A. Tight and Compact MILP Formulation for the Thermal Unit Commitment Problem. IEEE Transactions on Power Systems 2013 Nov;28(4):4897-4908. doi: 10.1109/TPWRS.2013.2251373.
[4] Knueven B, Ostrowski J and Watson JP. On Mixed-Integer Programming Formulations for the Unit Commitment Problem. INFORMS Journal on Computing 2020 Jun;32(4):857-876. doi: 10.1287/ijoc.2019.0944.
[5] Tejada-Arango DA, Lumbreras S, Sánchez-Martín P and Ramos A. Which Unit-Commitment Formulation is Best? A Comparison Framework. IEEE Transactions on Power Systems 2020 ;35(4):2926-2936. doi: 10.1109/TPWRS.2019.2962024.
[6] Zhong H, Liu Y, Yu Z, Yan X and Kang C. Efficient Optimization for Operation of Power Systems with High Proportion of Renewable Energy: A Review. CSEE Journal of Power and Energy Systems 2025 Nov;11(6):2794-2809. doi: 10.17775/CSEEJPES.2025.03200.
[7] Bunnak P, Coniglio S and Galelli S. Bridging Theory and Practice: Efficiently Solving the Unit Commitment Problem in Production Cost Models. Energy 2025 May;322:135454. doi: 10.1016/j.energy.2025.135454.
[8] Qu S and Yang Z. Infeasibility Cutting Plane for Unit Commitment Problem. CSEE Journal of Power and Energy Systems 2025 Nov;11(6):2639-2651. doi: 10.17775/CSEEJPES.2025.02790.
[9] Lezama-Lope UI, Ríos-Mercado RZ and Huerta-Muñoz DL. Enhancing Matheuristics for a Thermal Unit Commitment Problem Through Kernel Search and Local Branching. Computers & Operations Research 2026 May;189:107385. doi: 10.1016/j.cor.2026.107385.
[10] Pourahmadi F and Kazempour J. Unit Commitment Predictor With a Performance Guarantee: A Support Vector Machine Classifier. IEEE Transactions on Power Systems 2025 Jan;40(1):715-727. doi: 10.1109/TPWRS.2024.3400405.
[11] Venkatesh B, Shekeew MIA and Ma J. Feasibility-Guaranteed Machine Learning Unit Commitment: Fuzzy Optimization

Approaches. Applied Energy 2025 Feb;379:124923. doi: 10.1016/j.apenergy.2024.124923.

[12] Knueven B, Ostrowski J and Watson JP. Exploiting Identical Generators in Unit Commitment. IEEE Transactions on Power Systems 2018 Jul;33(4):4496-4507. doi: 10.1109/TPWRS.2017.2783850.

[13] Meus J, Poncelet K and Delarue E. Applicability of a Clustered Unit Commitment Model in Power System Modeling. IEEE Transactions on Power Systems 2018 Mar;33(2):2195-2204. doi: 10.1109/TPWRS.2017.2736441.

[14] Morales-España G and Tejada-Arango DA. Modeling the Hidden Flexibility of Clustered Unit Commitment. IEEE Transactions on Power Systems 2019 Jul;34(4):3294-3296. doi: 10.1109/TPWRS.2019.2908051.

[15] Koller M and Hofmann R. Efficient Clustering of Identical Generating Units for the MILP-UC with a Shifting Generation Level Method. Computers & Chemical Engineering 2019 Jun; 125:415-426. doi: 10.1016/j.compchemeng.2019.03.032.

[16] Palmintier BS and Webster MD. Heterogeneous Unit Clustering for Efficient Operational Flexibility Modeling. IEEE Transactions on Power Systems 2014 May;29(3):1089-1098. doi: 10.1109/TPWRS.2013.2293127.

[17] Du E, Zhang N, Kang C and Xia Q. A High-Efficiency Network-Constrained Clustered Unit Commitment Model for Power System Planning Studies. IEEE Transactions on Power Systems 2019;34(4):2498-2508. doi: 10.1109/TPWRS.2018.2881512.

[18] Zhang B, Ding T and Xiao Y. A Tight Unit Aggregation for Unit Commitment to Eliminate Symmetry. IEEE Transactions on Power Systems 2025 Nov;40(6):5264-5275. doi: 10.1109/TPWRS.2025.3578915.

[19] Tejada-Arango DA, Morales-España G, Wogrin S and Centeno E. Power-Based Generation Expansion Planning for Flexibility Requirements. IEEE Transactions on Power Systems 2020 May;35(3):2012-2023. doi: 10.1109/TPWRS.2019.2940286.

[20] Pourmoosavi MA and Amraee T. Low-Carbon Generation Expansion Planning Considering Flexibility Requirements for Hosting Wind Energy. IET Generation, Transmission & Distribution 2022 Jun;16(15):3153-3170. doi: 10.1049/gtd2.12506.

[21] Pourmoosavi MA and Amraee T. Stochastic Approaches to Sustainable Energy in Iran: Enhancing Power System Flexibility and Renewable Integration. Sustainable Energy Technologies and Assessments 2025 Feb;74:104145. doi: 10.1016/j.seta.2024.104145.

[22] Feng S, Wei W, Guo Z, Dong Z and Mei S. Solving Storage-Integrated Long-Term Unit Commitment With Guaranteed Bounds on Sub-Optimality. IEEE Transactions on Power Systems 2026 May;41(3):2219-2232. doi: 10.1109/TPWRS.2025.3638908.

[23] Najafi A. Input data for the tractable unit commitment formulation. GitHub repository; 2026. Available: https://github.com/afshinnajafii/Input-data-for-the-tractable-unit-commitment-formulation.